

# Effects of Porous Polystyrene Resin Parameters on *Candida antarctica* Lipase B Adsorption, Distribution, and Polyester Synthesis Activity

Bo Chen,<sup>†</sup> M. Elizabeth Miller,<sup>‡</sup> and Richard A. Gross<sup>\*,†</sup>

NSF I/UCRC for Biocatalysis and Bioprocessing of Macromolecules, Polytechnic University,  
6 Metrotech Center, Brooklyn, New York 11201, and Rohm and Haas Co., P.O. Box 904,  
Spring House, Pennsylvania 19477

Received December 5, 2006. In Final Form: March 2, 2007

Polystyrene resins with varied particle sizes (35 to 350–600  $\mu\text{m}$ ) and pore diameters (300–1000  $\text{\AA}$ ) were employed to study the effects of immobilization resin particle size and pore diameter on *Candida antarctica* Lipase B (CALB) loading, distribution within resins, fraction of active sites, and catalytic properties for polyester synthesis. CALB adsorbed rapidly (saturation time  $\leq 4$  min) for particle sizes  $\leq 120$   $\mu\text{m}$  (pore size = 300  $\text{\AA}$ ). Infrared microspectroscopy showed that CALB forms protein loading fronts regardless of resin particle size at similar enzyme loadings ( $\sim 8\%$ ). From the IR images, the fractions of total surface area available to the enzyme are 21, 33, 35, 37, and 88% for particle sizes 350–600, 120, 75, 35  $\mu\text{m}$  (pore size 300  $\text{\AA}$ ), and 35  $\mu\text{m}$  (pore size 1000  $\text{\AA}$ ), respectively. Titration with methyl *p*-nitrophenyl *n*-hexylphosphate (MNPHP) showed that the fraction of active CALB molecules adsorbed onto resins was  $\sim 60\%$ . The fraction of active CALB molecules was invariable as a function of resin particle and pore size. At  $\sim 8\%$  (w/w) CALB loading, by increasing the immobilization support pore diameter from 300 to 1000  $\text{\AA}$ , the turnover frequency (TOF) of  $\epsilon$ -caprolactone ( $\epsilon$ -CL) to polyester increased from 12.4 to 28.2  $\text{s}^{-1}$ . However, the  $\epsilon$ -CL conversion rate was not influenced by changes in resin particle size. Similar trends were observed for condensation polymerizations between 1,8-octanediol and adipic acid. The results herein are compared to those obtained with a similar series of methyl methacrylate resins, where variations in particle size largely affected CALB distribution within resins and catalyst activity for polyester synthesis.

## Introduction

*Candida antarctica* Lipase B (CALB) is attracting increased attention as a biocatalyst for chemical synthesis. This enzyme exhibits a high degree of selectivity over a broad range of substrates.<sup>1–4</sup> By enzyme immobilization, catalysts can be developed with significant advantages relative to free enzyme. For example, enzyme immobilization is well-known to improve enzyme thermal stability, activity, and recyclability.<sup>5</sup> Therefore, enzyme immobilization is critical to improving biocatalyst performance. Hydrophobic binding of lipases by adsorption has proved successful due to its affinity for water/oil interfaces. Furthermore, if the lipase has poor solubility in substrate–solvent reaction systems, minimal leakage (i.e., desorption) of lipases in nonaqueous media may be attained.<sup>6</sup> Many literature reports describe the high utility of immobilized CALB for chemical transformations of low molar mass compounds.<sup>3,7</sup> More recently, immobilized CALB has been shown to efficiently catalyze lactone ring-opening and condensation polymerizations.<sup>8–13</sup> Many of

these publications<sup>1,8–13</sup> describing CALB-catalyzed syntheses of low molar mass and polymeric molecules use commercially available immobilized CALB marketed by Novozymes as Novozym 435. This catalyst consists of CALB physically immobilized onto a macroporous acrylic polymer resin (Lewatit VP OC 1600, Bayer).

Both the nature of protein–surface interactions and the inherent properties of a specific enzyme will contribute to the catalytic activity of an immobilized biocatalyst. Adsorption of an enzyme onto a surface can induce conformational changes which affect the rate and specificity of the catalyst.<sup>14</sup> The total amount of enzyme loading, enzyme distribution within the immobilization support, and microenvironment surrounding the supported enzyme can all influence enzyme–catalyst activity, specificity, and stability.<sup>9,10,15,16</sup>

Immobilization research has largely focused on matrix selection and on optimizing immobilization conditions.<sup>17–28</sup> For example,

\* To whom correspondence should be addressed. Telephone: 718-260-3024. Fax: 718-260-3075. E-mail: rgross@poly.edu.

<sup>†</sup> Polytechnic University.

<sup>‡</sup> Rohm and Haas Co.

- (1) Gross, R. A.; Kumar, A.; Kalra, B. *Chem. Rev.* **2001**, *101* (7), 2097–2124.
- (2) Patel, R. N.; Banerjee, A.; Ko, R. Y.; Howell, J. M.; Li, W. S.; Comezoglu, F. T.; Partyka, R. A.; Szarka, F. T. *Biotechnol. Appl. Biochem.* **1994**, *20*, 23–33.
- (3) Kirk, O.; Christensen, M. W. *Org. Process Res. Dev.* **2002**, *6* (4), 446–451.
- (4) Kirk, O.; Björklund, F.; Godtfredsen, S. E.; Larsen, T. O. *Biocatalysis* **1992**, *6*, 127–134.
- (5) Kumar, A.; Gross, R. A.; Jendrosseck, D. *J. Org. Chem.* **2000**, *65* (23), 7800–7806.
- (6) Anderson, E. M.; Larsson, K. M.; Kirk, O. *Biocatal. Biotransform.* **1998**, *16*, 181–204.
- (7) Mahapatro, A.; Kumar, A.; Kalra, B.; Gross, R. A. *Macromolecules* **2004**, *37* (1), 35–40.
- (8) Sarda, L.; Desnuelle, P. *Biochim. Biophys. Acta* **1958**, *30*, 513–521.
- (9) Pieterse, W. A.; Vidal, J. C.; Volwerk, J. J.; de Haas, G. H. *Biochemistry* **1974**, *13*, 1455–1460.

- (10) Svendsen, A.; Clausen, I. G.; Patkar, S. A.; Kim, B.; Thellersen, M. *Methods Enzymol.* **1997**, *284*, 317–340.
- (11) Hu, J.; Gao, W.; Kulshrestha, A.; Gross, R. A. *Macromolecules* **2006**, *39*, 6789.
- (12) van der Mee, L.; Helmich, F.; de Bruijn, R.; Vekemans, J. A. J. M.; Palmans, A. R. A.; Meijer, E. W. *Macromolecules* **2006**, *39*, 5021.
- (13) Peeters, J.; Palmans, A. R. A.; Veld, M.; Scheijen, F.; Heise, A.; Meijer, E. W. *Macromolecules* **2004**, *37*, 1862.
- (14) Roach, P.; Farrar, D.; Perry, C. C. *J. Am. Chem. Soc.* **2005**, *127*, 8168–8173.
- (15) Wannerberger, K.; Arnebrant, T. *Langmuir* **1997**, *13* (13), 3488–3493.
- (16) Dyal, A.; Loos, K.; Noto, M.; Chang, S. W.; Spagnoli, C.; Shafi, K. V. P. M.; Ulman, A.; Cowman, M.; Gross, R. A. *J. Am. Chem. Soc.* **2003**, *125*, 1684–1685.
- (17) Dessouki, A. M.; Atia, K. S. *Biomacromolecules* **2002**, *3*, 432–437.
- (18) Maury, S.; Buisson, P.; Pierre, A. C. *Langmuir* **2001**, *17*, 6443–6446.
- (19) Soellner, M. B.; Dickson, K. A.; Nilsson, B. L.; Raines, R. T. *J. Am. Chem. Soc.* **2003**, *125*, 11790–11791.
- (20) Duracher, D.; Elaissari, A.; Mallet, F.; Pichot, C. *Langmuir* **2000**, *16*, 9002–9008.
- (21) Lei, C.; Shin, Y.; Liu, J.; Ackerman, E. J. *J. Am. Chem. Soc.* **2002**, *124*, 11242–11243.

work has addressed support surface hydrophobicity<sup>24–25</sup> and enzyme solution pH.<sup>27,28</sup> The influence of support physical parameters has also been studied. For example, by decreasing the particle size of a macroporous carrier, both the loading and specific activity of penicillin-G acylase increased.<sup>29</sup> Vertegel and Dordick reported that, relative to larger particles, adsorption of lysozyme onto nanoparticles resulted in less loss of lysozyme  $\alpha$ -helicity and higher catalytic activity.<sup>30</sup> CALB, adsorbed onto octyltriethoxysilane functionalized mesoporous silica, gave high enzyme loading (200 mg of protein/g of silica) and activity for the acylation of lauric acid with ethanolamine.<sup>31</sup> The excellent catalytic properties of this system were attributed to the support's high porosity and hydrophobic character. Our laboratory physically adsorbed CALB onto commercially available macroporous supports that differed in surface composition, hydrophobicity, pore diameter, and surface area. CALB–matrix systems with relatively higher activity for polyester synthesis had (i) CALB distributed throughout the matrix and (ii) an increased density of CALB molecules within the matrix pores.<sup>32</sup>

Previous studies generally did not consider enzyme distribution within carriers. However, this information can be of great value when seeking to better understand differences in enzyme activity observed by changing immobilization matrix parameters. For example, knowledge that an enzyme is primarily located within the outer regions of an immobilization support instead of being uniformly distributed throughout the matrix enables meaningful calculations of enzyme density along matrix surfaces as well as improved predictive models of substrate/product diffusion to and from immobilized protein. van Roon et al.<sup>33</sup> quantitatively determined the intraparticle distribution of Assemblase using light microscopy. They sectioned the matrix, and penicillin-G acylase was labeled with specific antibodies. The enzyme was heterogeneously distributed, and its concentration was radius-dependent. Our laboratory used infrared microspectroscopy to analyze protein spatial distribution within macroporous polymer supports.<sup>34</sup> By using a synchrotron beam light source, spatial resolution to 5 by 5  $\mu\text{m}$  was achieved.<sup>32,34</sup> IR absorbance bands corresponding to CALB and the polymer matrix distinguished these two components and were used to generate semiquantitative maps of protein distribution throughout the matrix.

Macromolecular substrates provide significant challenges relative to small molecules due to their high solution viscosities that cause diffusion constraints, limiting catalytic rates. The particle and pore sizes of macroporous enzyme supports will largely determine the diffusion rates of substrates and products

to and from catalysts. This variable is particularly important when assessing catalytic supports for enzyme-catalyzed polymer synthesis and modification reactions. To our knowledge, systematic studies have not been reported on how macroporous resin particle and pore size influences enzyme activity.

Recently, our laboratory immobilized CALB on a series of methyl methacrylate resins with identical average pore diameter (250  $\text{\AA}$ ) and surface area (500  $\text{m}^2 \text{g}^{-1}$ ) but with varied particle size (35 to 560–710  $\mu\text{m}$ ).<sup>35</sup> CALB adsorbed more rapidly onto smaller beads. Infrared microspectroscopy revealed that CALB forms protein loading fronts for resins with particle sizes 560–710 and 120  $\mu\text{m}$ . In contrast, CALB appeared evenly distributed throughout the 35  $\mu\text{m}$  resins. Titration with methyl *p*-nitrophenyl *n*-hexylphosphate (MNPHP) showed that the fraction of active CALB molecules adsorbed onto resins was <50%. By increasing the loading of CALB from 0.9 to 5.7% (w/w) onto 35  $\mu\text{m}$  methyl methacrylate beads, an increase in the fraction of active CALB molecules from 30 to 43% was observed. Furthermore, by decreasing the immobilization support diameter, a regular increase in  $\epsilon$ -caprolactone ( $\epsilon$ -CL) conversion to polyester resulted. Similar trends were observed for condensation polymerizations between 1,8-octanediol and adipic acid.

In this paper, a series of close-to-spherical styrene/divinylbenzene (DVB) resins of varying particle size and pore diameter were employed as supports for noncovalent adsorptive attachment of CALB by hydrophobic interaction. The effect of matrix particle and pore size on CALB (i) adsorption isotherms, (ii) fraction of active sites, (iii) distribution within supports, and (iv) catalytic activity for  $\epsilon$ -CL ring-opening polymerizations and adipic acid/1,8-octanediol polycondensations is reported. Important differences in the above for CALB immobilized on methyl methacrylate and styrene/DVB resins were found. The lessons learned herein provide a basis to others that seek to design optimal immobilized enzyme catalysts for low molar mass and polymerization reactions.

## Experimental Procedures

**Materials.** *Candida antarctica* Lipase B (CALB) in the form of a spray dried powder was a kind gift of Novozymes (Bagsvaerd, Denmark). The SDS–PAGE analysis of an aqueous solution of this powder showed a single band with a molecular weight (33 kDa) corresponding to CALB. The macroporous polystyrene resins were kind gifts from Rohm and Haas Co. All chemicals were purchased from Sigma Chemical Co. in the highest available purity and were used without further purification.

**Adsorption.** The beads (0.3 g) were shaken in 30 mL of ammonium bicarbonate at pH 7.8 (ABC buffer, 5 mM) containing 30 mg of CALB after wetting with ethanol. After incubation, the carrier was filtered, washed with ABC buffer, and then dried over silica gel under reduced pressure for 1 day. The loading of CALB on the supports (mg CALB/g support) was calculated as previously described.<sup>35</sup>

**Enzyme-Catalyzed Ring-Opening Polymerization of  $\epsilon$ -Caprolactone.** The method herein is identical to that described elsewhere.<sup>35</sup> In summary, biocatalyst water contents were measured using an Aquastar C3000 titrator with Coulomat A and Coulomat C from EMscience. The water content of immobilized resin was controlled with a drying pistol in the range from 1.0 to 1.7 wt % for all polymerizations. Reactions were monitored by *in situ*  $^1\text{H}$  NMR experiments with the NMR probe at 70  $^\circ\text{C}$ .  $^1\text{H}$  NMR measurements were performed on a Bruker DPX 300 spectrometer. The chemical shifts in parts per million (ppm) for the  $^1\text{H}$  NMR spectra were referenced relative to tetramethylsilane (TMS, 0.00 ppm) as the internal reference.

(22) Gill, I.; Pastor, E.; Ballesteros, A. *J. Am. Chem. Soc.* **1999**, *121*, 9487–9496.

(23) Bastida, A.; Sabuquillo, P.; Armisen, P.; Fernandez-Lafuente, R.; Huguet, J.; Guisan, J. M. *Biotechnol. Bioeng.* **1998**, *58*, 486–493.

(24) Sigal, G. B.; Mrksich, M.; Whitesides, G. M. *J. Am. Chem. Soc.* **1998**, *120*, 3464–3473.

(25) Koutsopoulos, S.; van der Oost, J.; Norde, W. *Langmuir* **2004**, *20*, 6401–6406.

(26) Xu, K.; Klivanov, A. M. *J. Am. Chem. Soc.* **1996**, *118*, 9815–9819.

(27) Pancera, S. M.; Gliemann, H.; Schimmel, T.; Petri, D. F. S. *J. Phys. Chem. B* **2006**, *110*, 2674–2680.

(28) Fernandez-Lorente, G.; Fernandez-Lafuente, R.; Palomo, J. M.; Mateo, C.; Bastida, A.; Coca, J.; Haramboure, T.; Hernandez-Justiz, O.; Terreni, M.; Guisan, J. M. *J. Mol. Catal. B: Enzym.* **2001**, *11*, 649–656.

(29) van Roon, J. L.; Joerink, M.; Rijkers, M. P. W. M.; Tramper, J.; Schroën, C. G. P. H.; Beffink, H. H. *Biotechnol. Prog.* **2003**, *19*, 1510–1518.

(30) Vertegel, A. A.; Siegel, R. W.; Dordick, J. S. *Langmuir* **2004**, *20*, 6800–6807.

(31) Blanco, R. M.; Terreros, P.; Fernandez-Perez, M.; Otero, C.; Diaz-Gonzalez, G. J. *Mol. Catal. B: Enzym.* **2004**, *30*, 83–93.

(32) Nakaoki, T.; Mei, Y.; Miller, L. M.; Kumar, A.; Kalra, B.; Miller, M. E.; Kirk, O.; Christensen, M.; Gross, R. A. *Ind. Biotechnol.* **2005**, *1*, 126–134.

(33) van Roon, J.; Beffink, R.; Schroën, K.; Tramper, H. *Curr. Opin. Biotechnol.* **2002**, *13*, 398–405.

(34) Mei, Y.; Miller, L.; Gao, W.; Gross, R. *Biomacromolecules* **2003**, *4*, 70–74.

(35) Chen, B.; Miller, E. M.; Miller, L.; Maikner, J. J.; Gross, R. A. *Langmuir* **2007**, *23*, 1381–1387.

**Table 1.** Matrix Parameters and Loading of *Candida antarctica* Lipase B (CALB) on Styrenic Beads

resin	samples	avg pore size (Å)	particle diam (μm)	surface area (m <sup>2</sup> /g)	enzyme loading (wt %) <sup>a</sup>	enzyme loading (mg/m <sup>2</sup> )	efficiency (%) <sup>b</sup>
1	Amberlite XAD 1180	400	350–600	500	7.9	0.160	87
2	Amberchrom CG 300C	300	120	700	8.7	0.124	95
3	Amberchrom CG 300M	300	75	700	8.4	0.120	92
4	Amberchrom CG 300S	300	35	700	8.4	0.120	92
5	Amberchrom CG 1000S	1000	35	200	8.3	0.420	91

<sup>a</sup> Enzyme loading was determined as the weight of CALB units on the carriers divided by the total weight of immobilized enzyme including the CALB units and carriers. <sup>b</sup> Efficiency was determined as the ratio of the percent of CALB added on the carriers to the total enzyme used during immobilization.

**Enzyme-Catalyzed Condensation of Adipic Acid and 1,8-Octanediol.** The reaction flask containing adipic acid (2.92 g, 20.0 mmol), 1,8-octanediol (2.92 g, 20.0 mmol), and immobilized lipase (1 wt % CALB relative to total monomer weight) was placed into a 90 °C oil bath for 30 min to melt the monomers. After 2 h, vacuum was applied (10 mm Hg) to facilitate water removal. Aliquots of ~20 mg were removed at selected time intervals. Reactions were terminated by adding excess cold chloroform, removing the immobilized enzyme by filtration, and then washing the beads twice with chloroform to extract the remaining polymer. The molecular weights of the reaction products were determined by gel permeation chromatography (GPC).

**Imaging of Protein Distribution Using Infrared Microscopy.** The method here is identical to that described elsewhere.<sup>35</sup> In summary, spectra of sectioned beads embedded in paraffin wax were collected in the transmission mode from 4000 to 750 cm<sup>-1</sup> by infrared microscopy. The enzyme concentration was calculated from the peak area corresponding to CALB (1610–1670 cm<sup>-1</sup>) divided by that of each resin (1430–1500 cm<sup>-1</sup>). A Magna 860 Fourier transform infrared (FTIR) spectrometer (Thermo Nicolet) and Synchrotron light from Beamline U10B at the National Synchrotron Light Source (Brookhaven National Laboratory) were used for small beads (35 and 75 μm), while a Spotlight FTIR spectrometer (Perkin-Elmer) was used for larger beads (120 and 350–600 μm).

**Active-Site Titration of Immobilized Lipase in Hexane.** In a sealed vial, 2 mL of methyl *p*-nitrophenyl *n*-hexylphosphate (MNPHP) diethyl ether/hexane solution (*a*<sub>w</sub> = 0.75) was added to immobilized enzyme (50 mg). After a 16 h reaction at 25 °C with shaking, the solvent was removed by vacuum. The mixture was then washed twice with 2 mL of acetonitrile (AcCN), and the concentration of *p*-nitrophenol was determined by liquid chromatography/mass spectrometry (LC/MS). Afterward, the carriers were washed with AcCN, dried by vacuum, and then assayed for enzyme activity via ring-opening polymerization of ε-caprolactone for 30 min (see above). The method of inhibitor synthesis and titration was described in more detail elsewhere.<sup>35</sup>

## Results and Discussion

**Lipase Adsorption.** Styrenic resins with systematically varied physical properties were employed as supports for CALB immobilization (Table 1), and the rates of CALB adsorption were measured (Figure 1). The weight ratio of CALB to resin was set at 1/10 for all adsorption experiments. For polystyrene resin samples 2–4, each with 300 Å pore size, the saturation time for CALB adsorption was ≤4 min, making it difficult to compare their adsorption rates. Resins 4 and 5, both with 35 μm diameter beads, differ in pore size (300–1000 Å) and, therefore, resin surface area (700–200 m<sup>2</sup> g<sup>-1</sup>). Despite these differences, resins 4 and 5 showed similarly rapid CALB adsorption. Only when the polystyrene resin particle size was increased from 120 μm to 350–600 μm (pore size 400 Å) did the absorption rate show a large decrease with saturation at ~24 h. In contrast, with methyl methacrylate resins of similar pore (250 Å) and particle (35–120 μm) sizes,<sup>35</sup> the rate of CALB adsorption decreased to large extents as the resin particle size was increased. Furthermore,

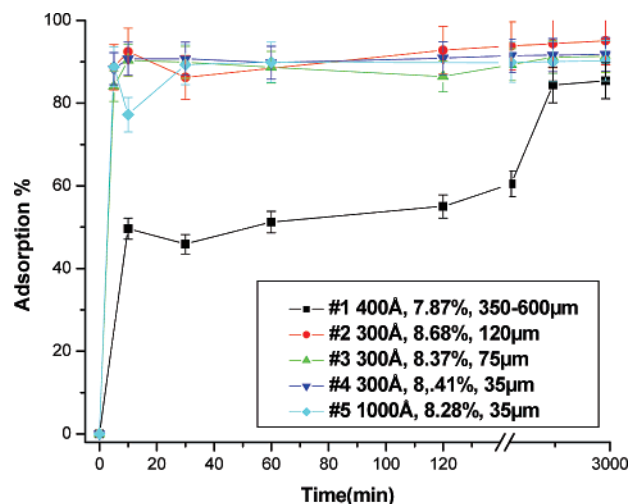


**Figure 1.** The isotherm of CALB adsorption as a function of time on different resins. Sample numbers correspond to the entries in Table 1.

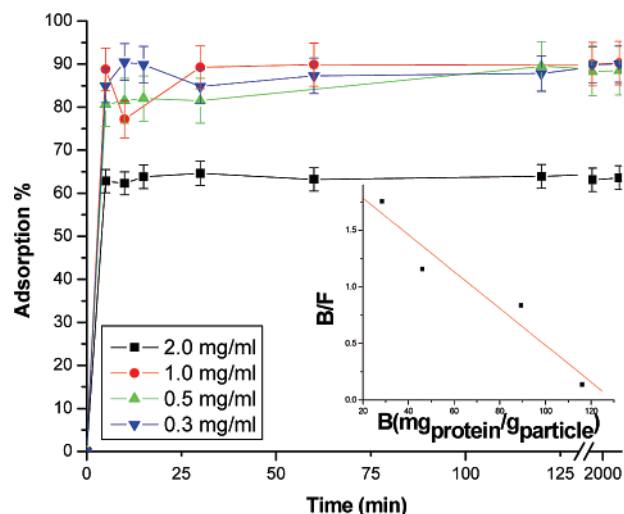
the loading saturation time for the 120 μm methyl methacrylate resin was ~300 min as opposed to ≤4 min. The enhanced adsorption rate of polystyrene resins relative to methyl methacrylate resins with similar physical parameters is attributed to stronger hydrophobic interactions between styrenic surfaces and CALB. The adsorption percent efficiency for polystyrene beads with sizes from 35 to 120 μm was 91–95% and decreased to 87% for the 350–600 μm support. Thus, with the exception of a small decrease in the enzyme loading wt % for the 350–600 μm diameter support, the total enzyme loading changed little for the series of polystyrene resins in Table 1.

Figure 2 shows that, when different enzyme concentrations were used for adsorption onto resin 5 (35 μm diameter, 1000 Å pore), in each case loading saturation was achieved in ≤4 min. Enzyme loading increased with increasing CALB concentration until the limiting adsorption was reached. Thus, by using 2.0 mg/mL CALB solution, the highest enzyme loading (0.53 mg/m<sup>2</sup>) was achieved, which corresponded to the lowest adsorption yield (65%). At relatively lower CALB solution concentrations, the yield remained constant at ~90%. The Scatchard analysis was used to determine the limiting adsorption of CALB onto 35 μm diameter, 1000 Å pore size polystyrene beads. In this method, linearization of the adsorption isotherm is achieved by using eq 1:

$$B/F = B_{\text{lim}}/C - B/C \quad (1)$$

where *B* is the weight (mg) of protein molecules bound to 1 g of resin beads, *F* is the concentration of native enzyme in μg/mL, *B*<sub>lim</sub> is the limiting adsorption given as the number of available adsorption sites per resin particle, and *C* is the constant for the dissociation of protein from the surface. This analysis gave values





**Figure 2.** Adsorption isotherms of CALB on Amberchrom CG 1000S with 35  $\mu\text{m}$  diameter using CALB solutions that differ in concentration. Inset: Linearization of the adsorption isotherm by using the Scatchard analysis to determine the limiting adsorption of CALB.  $B$  is the weight (mg) of protein molecules bound to 1 g of resin beads, and  $F$  is the concentration of native enzyme in micrograms per milliliter.

for  $B_{\text{lim}}$  and  $C$  of 141.4 mg/g (0.707 mg/m<sup>2</sup>) and 1.9  $\mu\text{M}$ , respectively. In comparison, a similar study with a 35  $\mu\text{m}$  diameter, 250  $\text{\AA}$  pore size poly(methyl methacrylate) resin gave a lower value for  $B_{\text{lim}}$  (71.8 mg/g, 0.144 mg/m<sup>2</sup>) and a higher value for  $C$  (3.9  $\mu\text{M}$ ). The  $B_{\text{lim}}$  value here means that enzyme was distributed throughout the macroporous resins. Thus, relative to methyl methacrylate, the polystyrene resin has a higher affinity for CALB. If CALB exists in its native conformation and forms a monolayer that completely covers the polystyrene surface, then enzyme loading would be 2.74 mg/m<sup>2</sup>. Since the experimental  $B_{\text{lim}}$  is  $\sim 25\%$  of the theoretical value for complete monolayer formation, and it is likely that CALB will tend to spread when adsorbed,<sup>35</sup> we conclude that the high affinity of CALB for polystyrene results in high surface coverage where CALB molecules are in close proximity along styrenic resin surfaces.

**Active Lipase Fraction.** Methyl *p*-nitrophenyl *n*-hexylphosphate (MNPHP) was selected as the inhibitor to determine, by titration, the fraction of catalytic sites that are accessible and active. Since we are concerned with CALB activity in organic media, inhibition was studied in heptane. LC-MS was used to determine the release of *p*-nitrophenol (*p*NP) which corresponds with accessible active sites. Further details on the method used are described in the Experimental Procedures and in ref 35. MNPHP-inhibited immobilized enzymes were used for  $\epsilon$ -caprolactone ring-opening polymerizations in toluene (70  $^{\circ}\text{C}$ ). No conversion of monomer was observed in 30 min. Hence, MNPHP titration resulted in complete inhibition of CALB activity.

Table 2 shows that CALB adsorption onto resins 1–5 results in  $>35\%$  deactivation of immobilized CALB molecules. This can be explained by enzyme denaturation and/or inaccessibility of active sites upon CALB adsorption to styrenic surfaces. At enzyme loadings of 7.9–8.7%, the fraction of active sites for immobilized CALB ranged from 57.7 to 64.2%. Thus, the fraction of active CALB molecules is independent of resin size for supports ranging from  $\sim 600$  to 35  $\mu\text{m}$ . Also, an increase in the pore size of the 35  $\mu\text{m}$  supports from 300 to 1000  $\text{\AA}$  (resins 4 and 5) at similar enzyme loadings ( $\sim 8\%$ ) had no effect on the fraction of active CALB molecules. Thus, the increase in the density of CALB molecules along the surface from 0.120 to 0.420 mg/m<sup>2</sup> does not appear to influence the availability of active sites. This

**Table 2.** *Candida antarctica* Lipase B (CALB) Immobilization on Styrene Resins of Differing Particle Size and Pore Size: Enzyme Loading, Fraction of Active Lipase, and Catalytic Activity

resin	protein loading (wt %)	water content (wt %)	reaction constant ( $\pm 6\%$ )	active site titration: fraction of active lipase (%)	TOF (s <sup>-1</sup> ) <sup>a</sup>
1	7.9	1.7	0.0090	57.7 $\pm$ 4.7	10.9
2	8.7	1.7	0.0095	61.3 $\pm$ 5.4	14.2
3	8.4	1.2	0.0090	64.2 $\pm$ 4.3	12.4
4	8.4	1.0	0.0093	62.5 $\pm$ 4.5	12.4
5	8.3	1.2	0.0225	63.2 $\pm$ 5.0	28.2 <sup>a</sup>

<sup>a</sup> Defined as the number of  $\epsilon$ -caprolactone molecules reacting per active site per second during the course of 30 min in ring-opening polymerizations performed at 70  $^{\circ}\text{C}$  in toluene.

**Table 3.** *Candida antarctica* Lipase B (CALB) Immobilization on Resin 5 with 5  $\mu\text{m}$  Diameter Beads: Effect of CALB Loading on the Fraction of Active Lipase and Catalyst Activity

enzyme loading (wt %)	enzyme loading (mg/m <sup>2</sup> )	water content (wt %)	reaction constant ( $\pm 6\%$ )	active site titration: fraction of active lipase (%)	TOF (s <sup>-1</sup> )
2.8	0.14	1.0	nd <sup>a</sup>	59.2 $\pm$ 3.2	nd <sup>a</sup>
4.4	0.21	1.2	0.0220	62.5 $\pm$ 3.6	25.7
8.3	0.42	1.2	0.0225	63.2 $\pm$ 5.0	28.2
10.6	0.53	1.1	0.0225	62.7 $\pm$ 4.8	31.0

<sup>a</sup> Not determined (nd) since good resolution in NMR experiments could not be achieved due to the large amount of resins added.

was further evaluated by increasing the enzyme loading on resin 5 from 2.8 to 10.6 wt %, giving enzyme densities along the resin surface of 0.14–0.53 mg/m<sup>2</sup>. The increase in enzyme density had no significant effect on the fraction of active lipase or turnover frequency for  $\epsilon$ -CL ring-opening polymerization (see Table 3). These results are reasonable given that  $B_{\text{lim}}$ , the number of available adsorption sites per resin particle, is 0.707 mg/m<sup>2</sup>. Hence, there is a sufficient availability of adsorption sites so that the microenvironment around CALB molecules may be similar at CALB densities of 0.120–0.53 mg/m<sup>2</sup>. In contrast, the fraction of active CALB molecules was 40–45% when CALB was immobilized on poly(methyl methacrylate) resins with similar particle and pore size values.<sup>35</sup> Hence, styrenic resins not only have a high affinity for CALB adsorption but also provide CALB with a surface environment that enables CALB to orient and take on conformations that retain a high degree of catalyst active site reactivity. It may be that the strong hydrophobic interactions that drive rapid CALB adsorption onto styrene/DVB resin surfaces are sufficiently robust to discourage the formation of CALB–CALB aggregates along surfaces at increased CALB loading. If such aggregates were to form and if the relative population of isolated and aggregated CALB molecules was to change with increased enzyme loading, then changes in enzyme conformation would be expected that would likely lead to shifts in CALB activity and the fraction of active CALB molecules.

#### Enzyme Distribution by Infrared (IR) Microspectroscopy.

Figure 3 displays IR images of protein distribution for CALB on styrene/DVB resins 1–5 at the protein loadings given in Table 1. The IR images show the formation of protein loading fronts that vary in thickness as a function of the resin physical parameters. The formation of a protein loading front was also observed by IR microspectroscopy for CALB physically immobilized on Lewatit (i.e., Novozym 435).<sup>32,34</sup> The enzyme entered the center of resin 5 (35  $\mu\text{m}$ , 1000  $\text{\AA}$  pore size) when enzyme loading was increased from 2.8 to 4.4, 8.3, and 10.6% (Figure 4). CALB diffused throughout resin 5 and the 35  $\mu\text{m}$  (250  $\text{\AA}$  pore size) poly(methyl methacrylate) beads when the enzyme loading was close to 10.6 and 5.7%, respectively. The

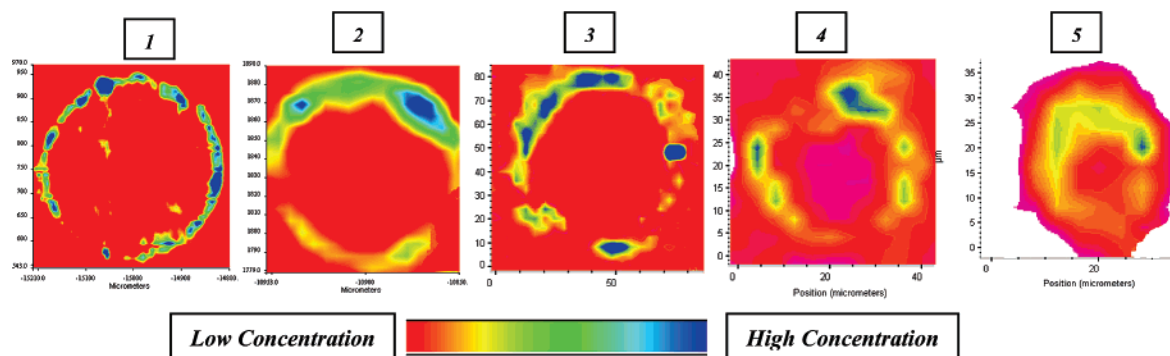


**Figure 3.** Distribution of CALB as a function of the matrix variables by IR microscopy. Synchrotron light source was only used on the images of 3 (75  $\mu\text{m}$ ), 4 (35  $\mu\text{m}$ ), and 5 (35  $\mu\text{m}$ ). Samples numbers correspond to the entries in Table 1.

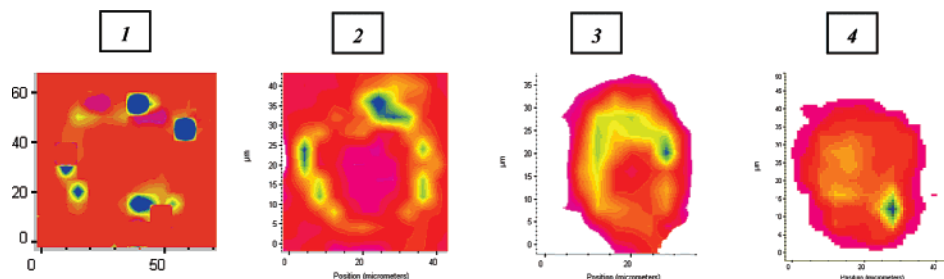


**Figure 4.** Distribution of CALB as a function of enzyme loading on Amberchrom CG 1000S by IR microscopy. Synchrotron light source was used on all the images. Sample numbers 1–4 correspond to the enzyme loading entries (2.8, 4.4, 8.3, and 10.6%, respectively) in Table 1.

thickness of the protein loading fronts for these beads was determined by first assuming that CALB is homogeneously distributed over a spherical zone within the resin beads. The values for the thickness of the spherical zone where CALB resides were determined from IR microspectroscopy imaging (see above). For resins with particle sizes 350–600, 120, 75, 35  $\mu\text{m}$  (pore size 300  $\text{\AA}$ ), and 35  $\mu\text{m}$  (pore size 1000  $\text{\AA}$ ), the thickness values are 30, 15, 10, 5, and 10  $\mu\text{m}$ , respectively. The surface area occupied by CALB was then calculated using eq 2:

$$S = A[1 - (d - 2b)/d]^3 \quad (2)$$

where  $S$  is the surface area occupied by CALB,  $A$  is the total surface area of the particles,  $b$  is the thickness within the particles occupied by CALB, and  $d$  is the particle diameter. From eq 2, for resins with particle sizes 350–600, 120, 75, 35  $\mu\text{m}$  (pore size 300  $\text{\AA}$ ), and 35  $\mu\text{m}$  (pore size 1000  $\text{\AA}$ ), CALB is distributed over surface areas of approximately 90, 230, 245, 260, and 175  $\text{m}^2$ , respectively. For resins 1–5, this corresponds to values of percent total surface area available to the enzyme of 21, 33, 35, 37, and 88%, respectively. Thus, at CALB loadings of  $\sim 8\%$  for resins 1–4,  $>60\%$  of resin surfaces are devoid of catalyst (see Table 1). In contrast, resin 5 is largely occupied by the enzyme. Resins 1–4 have similar surface areas at which CALB is found ( $\sim 250 \text{ m}^2$ ), loading ( $\sim 8.5\%$ ), enzyme density along surfaces, and percent area of beads at which CALB is found. The relatively greater ability of CALB to diffuse further into the interior regions of the 35  $\mu\text{m}$  polystyrene beads when the pore size was increased from 300 to 1000  $\text{\AA}$  (see images 4 and 5 in Figure 3) largely increased the percent area of beads at which CALB is found (37–88%).

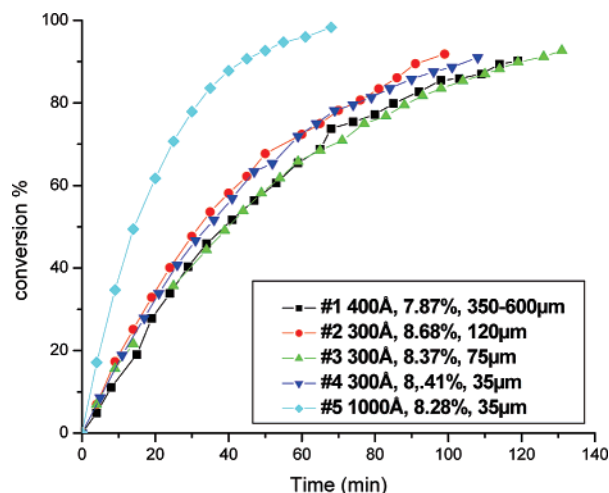
For comparison, the same analysis as above was performed using previously published data by our laboratory for CALB immobilized on a similar series of poly(methyl methacrylate) (PMMA) resins with an average pore size of 250  $\text{\AA}$ .<sup>35</sup> Decreases in PMMA resin particle size from 560 to 710 to 120, 75, and 35  $\mu\text{m}$  resulted in large changes in protein distribution. As a consequence, the percent accessible areas of CALB on PMMA

resins with particle sizes 560–710, 120, 75, and 35  $\mu\text{m}$  were approximately 51, 81, 95, and 100%, respectively. That is, as the resin size decreased, CALB diffused throughout the bead. Even 120  $\mu\text{m}$  PMMA beads had a large extent of CALB within the internal bead regions. These differences in protein distribution, and their relationship to catalyst activity, will be discussed below. The origin of the deviations in protein distribution between styrenic and PMMA resins is primarily attributed to the relatively higher affinity of CALB for the former. Lower affinity interactions between CALB and PMMA result in better diffusion of CALB within the resins to regions further within the beads.

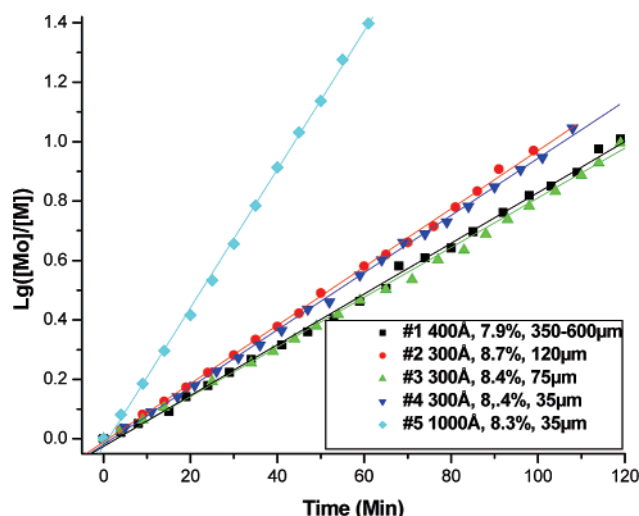
**Immobilized CALB Activity.** The activity of CALB immobilized on resins 1–5 (see Table 1) was assessed by  $\epsilon$ -CL ring-opening polymerizations. All immobilized resins have similar CALB loading (7.9–8.7 wt %) and water content (1.0–1.7%). As shown previously,<sup>35</sup> different chemical shifts are observed for methylene protons ( $-\text{OCH}_2-$ ) of the  $\epsilon$ -CL monomer, PCL internal repeat units, and chain terminal  $-\text{CH}_2-\text{OH}$  moieties. Hence, by *in situ* NMR monitoring, the monomer conversion and polymer number average molecular weight ( $M_n$ ) were determined.

Figure 5 illustrates that the polymerization rate is independent of resin diameter. During 30 min reactions, CALB immobilized on resins 1–4 gives a turnover frequency (TOF) of  $\epsilon$ -CL of  $\sim 12 \text{ s}^{-1}$ . In contrast, our previous work of CALB immobilized on PMMA resins showed a large dependence of  $\epsilon$ -CL percent conversion on resin particle diameter. For example, in 30 min reaction time, as the particle size decreased from 560–710, 120, 75, and 35  $\mu\text{m}$ , the turnover frequency (TOF) of  $\epsilon$ -CL increased from 3.8 to 5.3, 7.5, and 11.2, respectively. However, by increasing the resin pore size from 300 (resin 4) to 1000  $\text{\AA}$  (resin 5) for the 35  $\mu\text{m}$  beads, the TOF reached  $28.2 \text{ s}^{-1}$ . As discussed above, increase in resin pore diameter also corresponds to an increase in the percent area of beads at which CALB is found (37–88%).

Plots of  $\log([M]_0/[M]_t)$  versus time were constructed and are displayed in Figure 6. All plots in Figure 6 demonstrate a linear



**Figure 5.** Conversion rate of CALB as a function of the matrix variables. Sample numbers correspond to the entries in Table 1.



**Figure 6.** Reaction constants of immobilized resins as a function of the matrix variables in ring-opening polymerization.

relationship with correlation coefficients  $> 0.99$ . Thus, regardless of matrix particle size, monomer conversion followed a first-order rate law and termination reactions did not occur. Similar behavior was observed for  $\epsilon$ -CL ring-opening polymerizations catalyzed by CALB immobilized on Lewatit and a series of poly(methyl methacrylate) resins.<sup>35–40</sup> The activity of CALB catalysts immobilized on polystyrene resins was quantified by determining reaction kinetic constants ( $k_{app}$ ) by taking the slopes of  $\log([M]_0/[M])$  versus time plots. Changes in resin particle size gave kinetic constants that were nearly identical ( $0.0090$ – $0.0095 \text{ min}^{-1}$ ). However, increasing the pore size of the  $35 \mu\text{m}$  beads from  $300$  to  $1000 \text{ \AA}$  resulted in a large increase in the reaction kinetic constant ( $0.0093$  to  $0.0225 \text{ min}^{-1}$ ). Plots of  $M_n$  versus percent  $\epsilon$ -CL conversion were constructed and are displayed in Figure 7. Since the water content in the reactions is similar, the total number of propagating PCL chains should also be similar for CALB immobilized on resins 1–5. Hence, this explains that  $M_n$  at fixed monomer conversion values changed little as a function of resin size. Similar experiments performed for CALB im-

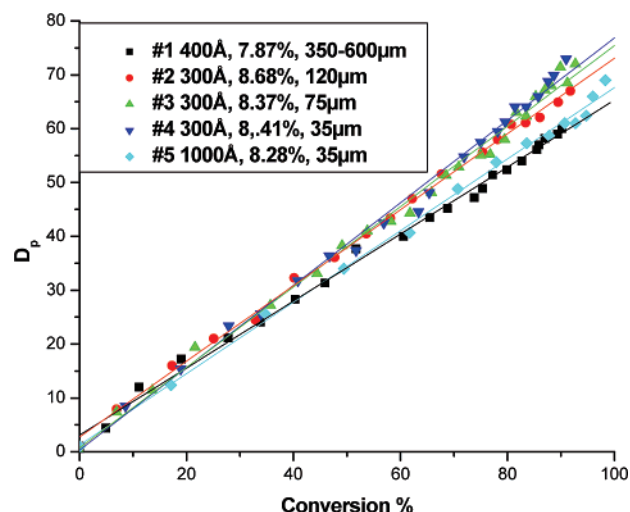


**Figure 7.** Degree of polymerization as a function of conversion. Sample numbers correspond to the entries in Table 1.

mobilized on PMMA supports also showed no significant effect of resin particle size on PCL  $M_n$  values.<sup>35</sup>

When CALB was immobilized on PMMA resins of constant pore size ( $250 \text{ \AA}$ ), as the particle size decreased from  $560$ – $710$ ,  $120$ ,  $75$ , and  $35 \mu\text{m}$ ,  $k_{app}$  increased from  $0.0012$  to  $0.0024$ ,  $0.0033$ , and  $0.0057 \text{ (min}^{-1}\text{)}$ , respectively. This trend, where the reaction rate increases as particle size decreases, would be expected if decreased particle size significantly increased the frequency of collisions between the substrates and CALB by decreasing the constraints for substrate and product diffusion to and from the immobilized enzyme. Since the fraction of active CALB molecules is not influenced by particle size when CALB is immobilized on either polystyrene or PMMA (see Table 1 and ref 31), the accessibility of active sites does not provide an explanation for the different responses observed for CALB activity as a function of particle size on polystyrene and PMMA supports.

Polymerizations of  $\epsilon$ -CL were performed using CALB immobilized on polystyrene resin 5 ( $35 \mu\text{m}$ ,  $1000 \text{ \AA}$ ) with CALB loadings of  $4.4\%$  ( $0.21 \text{ mg/m}^2$ ),  $8.3\%$  ( $0.42 \text{ mg/m}^2$ ), and  $10.6\%$  ( $0.53 \text{ mg/m}^2$ ). Catalyst quantities were adjusted so that polymerizations with these resins were performed with a CALB to  $\epsilon$ -CL weight ratio of  $0.01$ . Inspection of Figure 8 shows no significant change in the polymerization rate as a function of enzyme loading. As the enzyme loading on resin 5 increased from  $4.4$  to  $8.3$  and  $10.6\%$ , the  $\epsilon$ -CL turnover frequencies (TOF) during the initial  $10 \text{ min}$  of reactions were  $25.7$ ,  $28.2$ , and  $31.0 \text{ s}^{-1}$ , respectively. In addition, the reaction constants were also very similar ( $0.0220$ – $0.0225 \text{ min}^{-1}$ ). This result is consistent with invariable CALB active site fractions with changes in CALB loading (see Table 3). However, when CALB was immobilized on a PMMA resin of identical particle size ( $35 \mu\text{m}$ ) but of smaller pore size ( $250 \text{ \AA}$ ), large differences in CALB activity were observed as a function of CALB loading. Remarkably, during  $30 \text{ min}$  reactions using the PMMA support, as CALB loading increased from  $2.6$  to  $4.3$  and  $5.7\%$ , the TOF of  $\epsilon$ -CL increased from  $1.0$  to  $5.2$  and  $11.2 \text{ s}^{-1}$ , respectively. This nonlinear relationship between enzyme concentration and reaction rate can partially be explained by the increased fraction of active sites with increased CALB loading (see ref 35). Furthermore, an increase in enzyme loading on the PMMA resin resulted in a more uniform distribution of enzyme throughout the beads, which was shown previously to be beneficial to catalyst activity.

The activity of CALB immobilized on resins 1–5 was also assessed by condensation polymerizations of adipic acid and

(36) Mei, Y.; Kumar, A.; Gross, R. A. *Macromolecules* **2002**, *35*, 5444–5448.

(37) Deng, F.; Gross, R. A. *Int. J. Biol. Macromol.* **1999**, *25*, 153–159.

(38) Henderson, L. A.; Svirkin, Y. Y.; Gross, R. A.; Kaplan, D. L.; Swift, G. *Macromolecules* **1996**, *29*, 7759–7766.

(39) Matsumoto, M.; Odachi, D.; Kondo, K. *Biochem. Eng. J.* **1999**, *4*, 73–76.

(40) Mei, Y.; Kumar, A.; Gross, R. *Macromolecules* **2003**, *36*, 5530–5536.



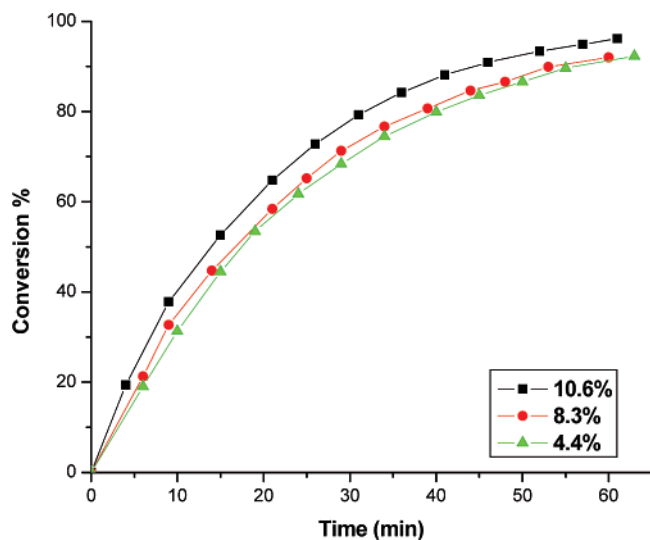


**Figure 8.** Effect of CALB loading (see legend box in plots) onto Amberchrom CG 1000S with a 35  $\mu\text{m}$  bead diameter on the time course for  $\epsilon$ -caprolactone ring-opening polymerizations at 70  $^{\circ}\text{C}$  in toluene.

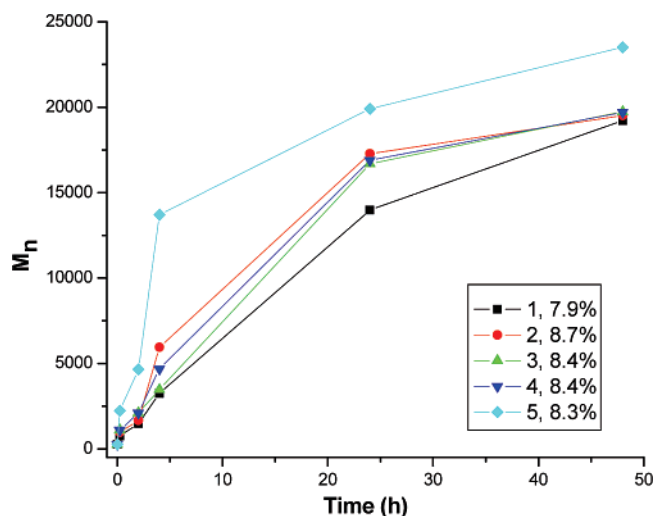


**Figure 9.** Immobilized CALB catalysis of adipic acid/1,8-octanediol condensation polymerization at 90  $^{\circ}\text{C}$  in bulk. Sample numbers correspond to the entries in Table 1.

1,8-octanediol (Figure 9). As above, all immobilized resins have similar CALB loading (7.9–8.7 wt %). As the particle size decreased from 350–600, 120, 75, and 35  $\mu\text{m}$  at a constant pore diameter, the plots of  $M_n$  versus reaction time were nearly identical. In contrast, CALB immobilized on a similar series of poly(methyl methacrylate) resins showed large increases in  $M_n$  as resin particle size was decreased.<sup>35</sup> However, by increasing the pore size of the 35  $\mu\text{m}$  beads from 300 to 1000  $\text{\AA}$ , a substantial increase in polyester molecular weight resulted. Large differences in polyester molecular weights were observed at short reaction times. For example, at 4 h, the poly(octanoyl adipate)  $M_n$  values for CALB immobilized on resins 4 and 5 were 2100 and 4700, respectively. As above for  $\epsilon$ -CL polymerizations, increased chain growth during poly(octanoyl adipate) synthesis as a result of increasing the pore size of 35  $\mu\text{m}$  polystyrene resins from 300 to 1000  $\text{\AA}$  is explained by an increased diffusion of the substrates and products to and from the immobilized enzyme.

From the above results on CALB activity as a function of particle size for polystyrene and PMMA resins, we believe that the percent surface area occupied by CALB is a critical factor that can be used to improve immobilized CALB activity. Increased

percent accessible surface area will increase the probability of collisions between substrates and CALB. As the percent accessible surface area for CALB increased for PMMA resins, a corresponding increase in polyester synthesis reaction rates was observed (see above). CALB immobilized on styrenic particles of variable size showed little differences in both percent accessible surface area and polyester synthesis catalyst activity. The potential benefit of decreasing bead particle size is to decrease diffusion constraints that lead to productive collisions between the enzyme and substrate. However, for this series of polystyrene resins, as particle size decreased, the percent resin area in which reactions can occur does not change. In contrast, decreasing PMMA particle size dramatically increased CALB coverage of available resin surfaces. Thus, as PMMA particle size is decreased, substrate and product diffusion in and out of particles increases along with the surfaces in which CALB is found. Increased catalyst activity for polystyrene resin 5 relative to 4 was achieved by increasing the pore size to 1000  $\text{\AA}$ . Increasing the resin particle surface area caused a large increase in the percent of resin occupied by CALB. Furthermore, by an increase in resin pore size, the limitations caused by substrate–product diffusion into and out of the resin will be eased. Compared to styrenic resin 4 with particle size 35  $\mu\text{m}$  and pore size 300  $\text{\AA}$ , the PMMA resin with particle size 35  $\mu\text{m}$  and pore size 250  $\text{\AA}$  has higher percent accessible surface area but lower activity. This can be explained by the fact that PMMA has (i) surfaces with relatively higher hydrophilicity that is unfavorable to CALB activation, (ii) smaller pore size, and (iii) a relatively lower fraction of active sites. This difference in available active sites is attributed to changes in CALB orientation on the respective surfaces. Work is currently ongoing to better define CALB orientation on these and other surfaces of interest.

## Summary of Results

CALB showed a high affinity for adsorption onto polystyrene resins. Except for the 350–600  $\mu\text{m}$  (pore size 400  $\text{\AA}$ ) resin, the saturation time for CALB adsorption was  $\leq 4$  min. In contrast, adsorption to methyl methacrylate resins occurred much more slowly.<sup>35</sup> For instance, the loading saturation time for a 120  $\mu\text{m}$  particle size methyl methacrylate resin was  $\sim 300$  min as opposed to  $\leq 4$  min for a 120  $\mu\text{m}$  polystyrene resin. The enhanced adsorption rate of polystyrene resins relative to methyl methacrylate resins with similar physical parameters is attributed to stronger hydrophobic interactions between the styrenic surfaces and CALB. The adsorption percent efficiency for polystyrene beads with sizes from 35 to 120  $\mu\text{m}$  was 91–95%. The above results were consistent with those from a Scatchard analysis that gave values for the limiting adsorption of CALB onto polystyrene and poly(methyl methacrylate) beads.

At enzyme loadings of 7.9–8.7%, the fraction of active sites for immobilized CALB on polystyrene resins ranged from 58 to 64%. The fraction of active CALB molecules is independent of polystyrene resin size for the range of supports studied herein. Furthermore, an increase in enzyme density had no significant effect on the fraction of active lipase or turnover frequency for  $\epsilon$ -CL ring-opening polymerizations. These results are attributed to a sufficient availability of adsorption sites on polystyrene resins so that the microenvironment around the CALB molecules is largely invariable for the polystyrene resins and CALB loadings studied herein. In contrast, when CALB was immobilized on poly(methyl methacrylate) resins with similar particle and pore size values, the fraction of active CALB molecules was 40–45%.<sup>35</sup> Therefore, styrenic resins both have high affinity for CALB adsorption and also provide CALB with

a surface environment that enables CALB to orient and take on conformations that retain a high degree of catalyst active site reactivity.

In contrast to a previous study with poly(methyl methacrylate) resins,<sup>35</sup> the  $\epsilon$ -CL conversion rate was not influenced by changes in resin particle size. We believe that an important contributing factor to this remarkable difference in the behavior of immobilized CALB is the variation in the distribution of CALB within the resins. The fraction of total surface area where CALB is found in resins was determined from IR microspectroscopy generated images. A high percent total surface area where CALB is found within the resins enables collisions between the substrate and CALB, leading to product formation. In contrast, resins with large areas devoid of CALB result in substrate diffusion within the resin regions where substrate–catalyst collisions cannot occur. For CALB immobilized on polystyrene, the catalytic activity was not influenced by particle size since this series of catalysts had similarly small ( $\sim 30\%$ ) fractions of surface areas where

CALB is found. In contrast, the activity of CALB on PMMA resins increased as particle size decreased which corresponds to large increases in the fraction of resin surface area where CALB was found.

**Acknowledgment.** The authors thank the NSF and Industrial members (BASF, Novozymes, Johnson & Johnson, Rohm and Haas, Genencor, Estée Lauder, DNA 2.0, W.R. Grace, Grain Processing Corporation, and DeGussa) of the NSF-Industry/University Cooperative Research Center (NSF I/UCRC) for Biocatalysis and Bioprocessing of Macromolecules at Polytechnic University for their financial support, intellectual input, and encouragement during the course of this research. We are also grateful to Dr. Lisa Miller and colleagues for providing access to the FTIR facilities at the National Synchrotron Light Source (Brookhaven National Laboratory, Upton, New York 11973).

LA063515Y